STARS

2021

Low-Profile Wireless Passive Temperature Sensors

Ectis Velazquez

University of Central Florida

LOW-PROFILE WIRELESS PASSIVE TEMPERATURE SENSORS

by

ECTIS VELAZQUEZ JR
B.S. University of Central Florida, 2017

A thesis submitted in partial fulfilment of the requirements
for the degree of Master of Science
in the Department of Electrical and Computer Engineering
in the College of Engineering and Computer Science
at the University of Central Florida
Orlando, Florida

Spring Term
2021

ABSTRACT

This thesis explores design challenges and promising solutions for temperature sensors for high temperature environments such as combustion turbines. To survive this high temperature environment of over 1000°C the sensors are required to be robust in their electrical and mechanical properties. Wire connections for these high temperature environments are a complex problem due to the physical limitations of most materials at those high temperatures. In this thesis, robust ceramic sensors based on microwave resonators are demonstrated for high temperature environments, with some studies into optimizing the techniques used to measure them, as well as the distance at which their responses can still be measured. Two types of temperature sensors are realized using rectangular reflective patches with different dielectric substrates. The sensors are realized with either alumina substrate or yttria-stabilized zirconia (YSZ), both of which have temperature dependent dielectric constants. The temperature is wirelessly detected by measuring the resonant frequency of the reflective patch. The reflective patch sensor works simultaneously as a resonator and a radiative element. The sensors were tested up to 800°C. In these high temperature environments, it is important to be able to interrogate the sensor from a distance safe for the interrogating antenna, for this reason, the sensors must be designed with a high enough Q factor that their responses can be measured up to at least 2 inches of distance away from the interrogating antenna. While exploring designs of temperature sensors, a few measurement techniques on the vector network analyzer are studied to optimize the identification of the resonant frequency of the reflective patches. These measurements include the start and stop time of the time domain gating window, the start and stop frequency of the frequency span of the interrogating signal, and the gain/size of the interrogating horn antenna.

I would like to dedicate this thesis to all of the incredible people I have been blessed to have in my life. Without all of you, none of this would be possible.

ACKNOWLEDGMENTS

TABLE OF CONTENTS

LIST OF FIGURES

LIST OF TABLES

CHAPTER 1: INTRODUCTION

In this chapter the background on the sensors for high temperature environment applications is introduced using reflective patch resonators. The design considerations and an overview of the thesis are presented.

1.1 Motivation

The motivation for this research is to create low-profile wireless sensors for use in combustion gas turbines. The sensors would look to be placed on turbine blades, whose temperatures can reach 1260°C [1]. The turbine is composed of an array of alternating stationary and rotating blades. As the combustion gas expands through the turbine, it spins the rotating blades, which spin a generator which produces electricity. As described in [2], the performance of these turbines is dependent on maintaining optimal temperatures, and thus monitoring these temperatures has remained a complex problem to solve, since at these extreme temperatures there is no plethora of materials that can survive. A wireless solution, and one that can be implemented with minimal disruption to the operation of the turbine, seems to be the ideal way to monitor the temperature within the turbine.

1.2 Overview of Reflective Patch Sensors

From [2], the reflective patch sensor is based on the relationship between the resonant frequency of the reflective patch and the temperature of the dielectric material. It is both a radiative element and a resonator. This sensor's compact volume and planar structure allow for a low-profile application where the sensor can fit onto a combustion turbine blade. By using materials that can survive these harsh temperatures and a wireless passive sensing setup, the sensors are able to operate reliably at

elevated temperatures. Measurements are taken by wirelessly interrogating the resonant frequency f_r using an open-ended waveguide (OEWG) or horn antenna.

1.2.1 Principle of Reflective Patch as a Temperature Sensor

To avoid any potential conflicts with higher order modes, the resonators operate in the two fundamental modes, TM_{100} and TM_{010} modes. To keep consistent with the design from [2] the TM_{010} mode is used, however for the purposes of temperature sensing the mode chosen does not make any difference. For the TM_{010} mode, the resonant frequency is given by:

$$f_r = \frac{c}{2L_{eff}\sqrt{\epsilon_r}} \tag{1.1}$$

Where L_{eff} is the effective resonant length, ϵ_r is the relative permittivity of the patch dielectric substrate, and c is the speed of light in a vacuum. When the temperature rises, the dielectric constant of the dielectric substrate also rises [3], and because of this the resonant frequency f_r decreases monotonically. This means the temperature can be detected by measuring the resonant frequency, and the change in it. The wireless interrogation is done by using different OEWGs and horn antennas to send wideband microwave signals to excite the patch sensor's TM_{010} mode. The sensor receives this signal, uniform in the frequency domain, and then re-radiates a modulated microwave signal at the resonant frequency. This can be identified by reading the S_{11} frequency response after gating in the time domain, by reading the resonant peak due to the reflective patch.

1.3 Design Considerations

There are a few design considerations that must be taken into account before beginning to test different dielectrics and conductors. The designs must consider the patch dimensions, coupling condition, and substrate thickness. For this work, all substrate samples were created with set thicknesses. For operation as a temperature sensor, the reflective patch resonator should have a patch with dimensions designed for critical coupling. Under critical coupling, the S_{11} is zero at the resonant frequency. This is an important characteristic for the sensor because this ensures that because the response will be delayed, it will come after the reflections due to the environment and the physical structure of the interrogating antenna. Using Ansys High-Frequency Structure Simulator (HFSS), the reflective patch design from [2] is used as the base for the first designs and tests. This sensor used a reflective patch of resonant length $L = 9.3$mm, width (non-resonant dimension) $W = 8$mm, and dielectric substrate thickness $h = 0.625$mm. This design is simulated in HFSS, interrogated with an ideal parallel-plate waveguide and shown in Fig. 1.1.

These parameters were chosen to optimize the Q_T, total quality factor of the sensor and for it to operate at 4.7 GHz at 1000°C and 5.1 GHz at room temperature. From [4] the coupling is primarily governed by the relationship between Q_{rad} and the unloaded Q, Q_U. The relationship is described as:

- $Q_{rad} = Q_u$: critically-coupled

- $Q_{rad} > Q_u$: under-coupled

- $Q_{rad} < Q_u$: over-coupled
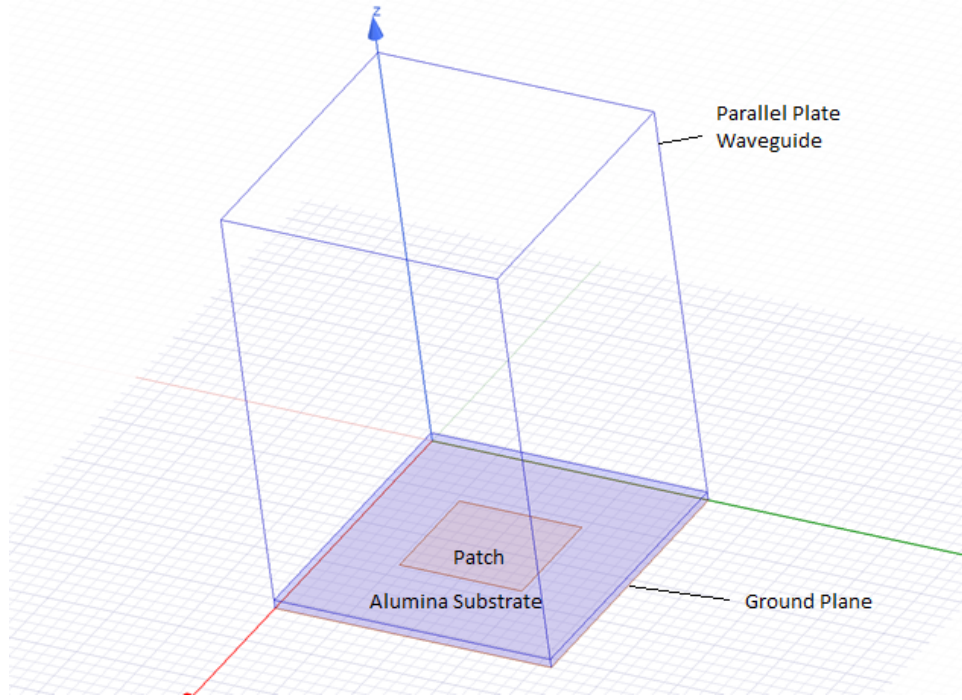
Figure 1.1: Sensor design in HFSS with parallel plate waveguide interrogation.

Q_T is calculated using the following relationship between the resonant frequency and the 3dB frequencies:

$$Q_T = \frac{f_r}{f2 - f1} \tag{1.2}$$

There are four parameters studied in [4] and how they affect coupling. three of these have to do with the dielectric substrate, the dielectric constant, ϵ_r, the loss tangent, $tan\delta$, and the substrate thickness, h. The last metric studied was the width, W, or the non-resonant length. Given that only two dielectrics are used in this work (YSZ and alumina), and that the samples are fabricated with fixed thicknesses, the only previously studied parameter that can be adjusted for design is the width, W. To fully optimize the design of the rectangular patch to achieve critical coupling, both of the dimensions are varied and the effects studied in simulation and a sweep is performed of each one as two separate tests. The results of varying the resonant length are shown in Fig. 1.2.

4
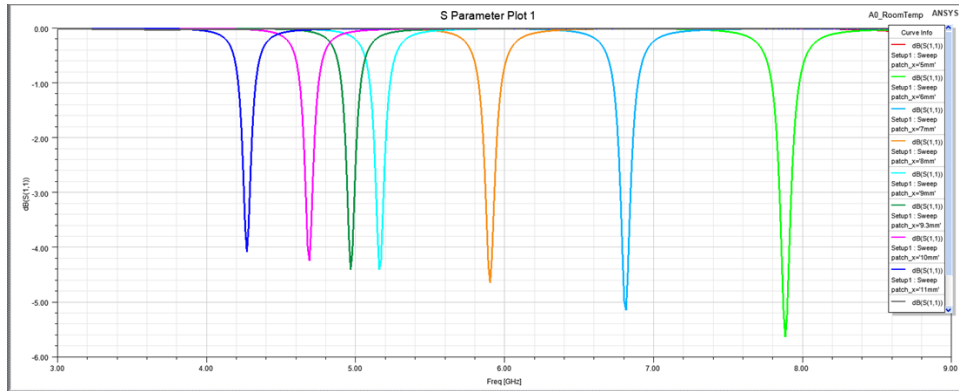
Figure 1.2: Resulting plot showing the effects of varying resonant length on the S_{11} response, primarily affecting resonant frequency

The resonant length is varied from 5mm to 12mm in increments of 1 mm while keeping the other dimension constant. This is done to get a more complete idea of the effects on the response of the sensor. From these results, the resonant length changes the resonant frequency, but has minimal effects on the coupling. The other dimension of the patch, W, is actually the one that has the greatest effect on the coupling, as shown in Fig. 1.3.
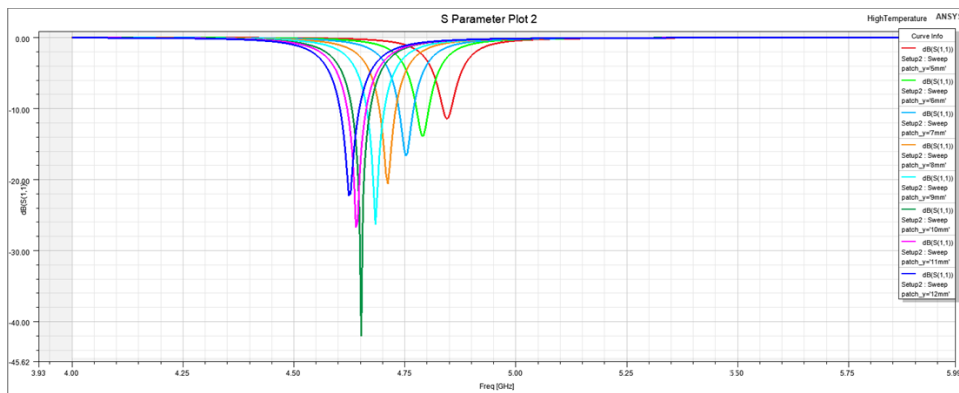
Figure 1.3: Resulting plot showing the effects of varying the non-resonant length on the S_{11} response. The different coupling conditions are shown as the width is changed.

Critical coupling is only achieved at one exact width, and between fabrication tolerances and pos-

5

sible material expansions and contractions with varying temperatures, there is no feasible way to guarantee that the sensor will have the width required for critical coupling. This is not an issue, as the goal is to minimize the S_{11} reflection coefficient at the resonant frequency. For this purpose, a target value of around -20dB is chosen, with values of -15dB also being acceptable. When the sensor response is simulated With this consideration, it can be seen that the patch dimensions actually have a lot of leeway to achieve a good enough coupling. Besides the patch dimensions, the resonant frequency is an important consideration. The vector network analyzer (VNA) operates from 300kHz to 20GHz. Because of this, the patch must not be made too small so that its fundamental mode does not resonate above 20GHz or too large that it resonates below 300 kHz. For an alumina substrate (bulk alumina dielectric constant of 9.2) 0.3 mm thick this would mean the resonant length of the patch can be no smaller than 2.5 mm and no larger than 164 meters. This further proves there is a great deal of room for possible designs of patch dimensions. The substrate samples were mostly fabricated as 1" x 1" (25mm x 25mm) or 2" x 2" (50mm x 50mm) squares, so the patch antennas must fit within these spaces.

1.4 Fabrication of Sample Substrates

The substrates used for sampling were fabricated with various different thicknesses and materials.

Fig. 1.4 shows the structures of the different samples fabricated. These samples were fabricated for the purposes of prototyping reflective patch sensors and testing them at different temperatures. Some samples were made to be 1" x 1" or 2" x 2" as they would fit perfectly into devices used for high temperature measurements. The samples used and their dielectric thicknesses are shown in Table 1.1
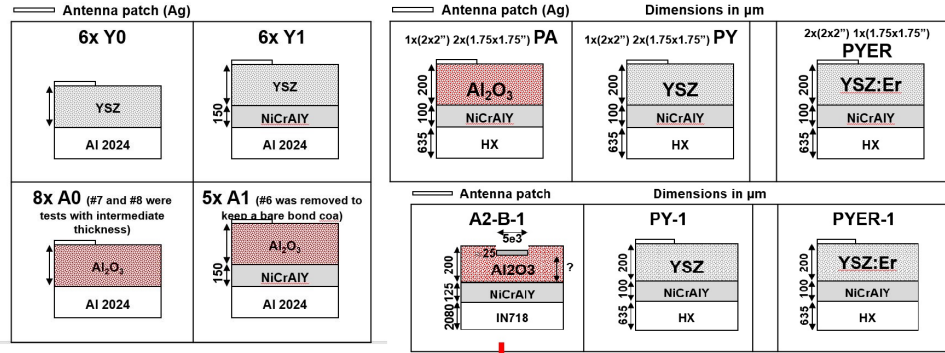
Figure 1.4: All samples fabricated for purposes of this work. the naming conventions describe the makeup of the samples.

Table 1.1: Sample names and the thicknesses of the dielectric substrates.

Sample	Thickness h [μm]
A0-4	295
A1-5	270
Y0-2	200
Y0-4	388
Y1-1	162
Y1-3	155
PA	200
PY	200
A3	500

Most of the samples were fabricated by physical vapor deposition. The dielectrics and the bond coat, originally powders, were deposited onto the metal substrates using an air plasma spray gun to create an even coating. [5] There is also another sensor, dubbed A3, that was fabricated by diffusion bonding platinum and alumina. Another set of resonators were made from Rogers 4003 dielectric. These patch resonators in Fig. 1.5 were designed to be high Q resonators that operate at resonant frequencies of 10GHz, 12GHz, and 14GHz. These were used primarily as standards to ensure a proper working measurement setup before the other sensors were tested.
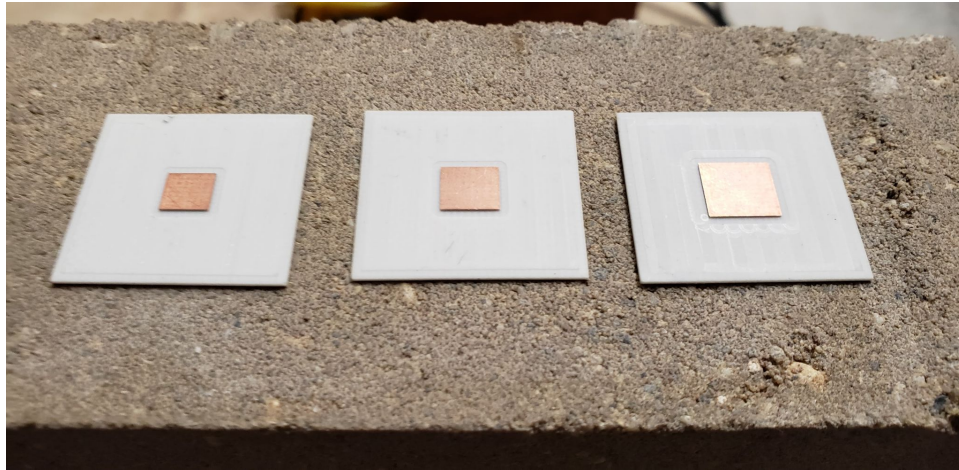
Figure 1.5: Picture showing the three Rogers 4003 resonators

1.5 Thesis Overview

In this thesis, ceramic sensors for high temperature measurements are presented using several different materials and design characteristics. The sensors are interrogated using waveguides and horn antennas at distances from 7mm to 300 mm to achieve wireless interrogation. Every step of the design builds upon the previous step, so each chapter can be thought of as chronological/sequentially ordered. Proper identification of the resonant peaks on the VNA is important and for that Chapter 2 explores the different measurement technique optimizations and the conclusions drawn from them. Chapter 3 begins with the designs of test sensors used for material characterization and proof of concept at room temperature. This includes the testing of YSZ as a dielectric material, comparing it to the alumina sensors, and the NiCrAlY bond coat as a bottom ground plane conductor in comparison to aluminum. Chapter 4 explores the high temperature design realizations for sensors using alumina and YSZ as the dielectric material, while also performing testing on the long distance limits for the sensors. Finally, Chapter 5 summarizes the thesis conclusions and suggests future work.

CHAPTER 2: MEASUREMENT OPTIMIZATION STUDY

Proper identification of the sensor response is the most important part of the measurement process. To optimize the methods used to interrogate the signal, several aspects of the measurement process are studied. This includes the time domain window used for gating, the frequency span observed on the VNA, and the gain and size of the interrogating horn antenna. For these studies, a Keysight ENA network analyzer is used. For the purposes of the measurements of the sensors, a Performance Network Analyzer (PNA) is used. This type of VNA gives up to 16001 points, which yields higher precision measurements.

2.1 Time Gating Window

Using a Rogers 4003 patch resonator that resonates at 12GHz, the effects of different time domain gating windows was studied. The start time was kept constant, as naturally the gating window must start after the reflections from the aperture of the interrogating antenna/waveguide. The stop time is the variable under test in this study. A tighter or wider window will have different effects on the signal response observed on the VNA. Fig. 2.1 shows the effects of different stop times on the response. If the gating window is too short, the signal and especially the peaks lose sharpness. If the signal is increased it increases the sharpness up to a certain point, after which the effects are no longer visible. In this case, this happens at around 5-10 ns. For the measurements described in this thesis, the gating windows were always made wide enough until the effects of increasing the window were no longer visible.
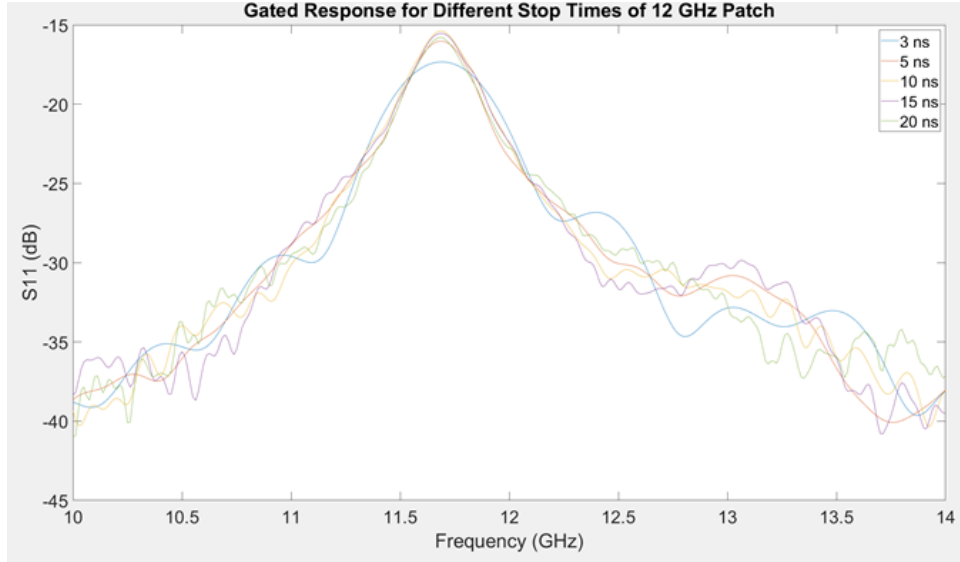
Figure 2.1: Comparison of different time domain gating window lengths. Start time 1 ns with end times varied.

2.2 Frequency Span

Another important parameter under study is the frequency span. By having a greater frequency span, the resolution of the inverse Fourier Transform (IFFT) in the time domain is increased, which appears to give sharper peaks in the VNA. The relationship between the frequency range and time domain resolution is described by:

$$\frac{1}{2f_{max}} \tag{2.1}$$

However, this does have an adverse effect on the measurement. The VNA shows 1601 points between the frequency span. If the frequency span is very long (300 kHz - 20GHz is the limit), then there will be fewer points between the peaks and the small frequency effects from temperature shifts will not be measurable. Using the same 12GHz resonator, and using a fixed time domain gating window from 1 - 10 ns, the frequency span that the VNA is calibrated for are varied. The results are shown in Fig. 2.2, which shows that although the VNA may appear to lose some sharpness

in the peak, the actual data is unaffected, and actually improved by a narrower frequency span. For the best identification of resonance and high temperature measurements, a wide frequency span is first used to quickly identify and confirm the resonant peak on the VNA display before calibrating for a narrower frequency span that will show the shift in frequency more clearly.
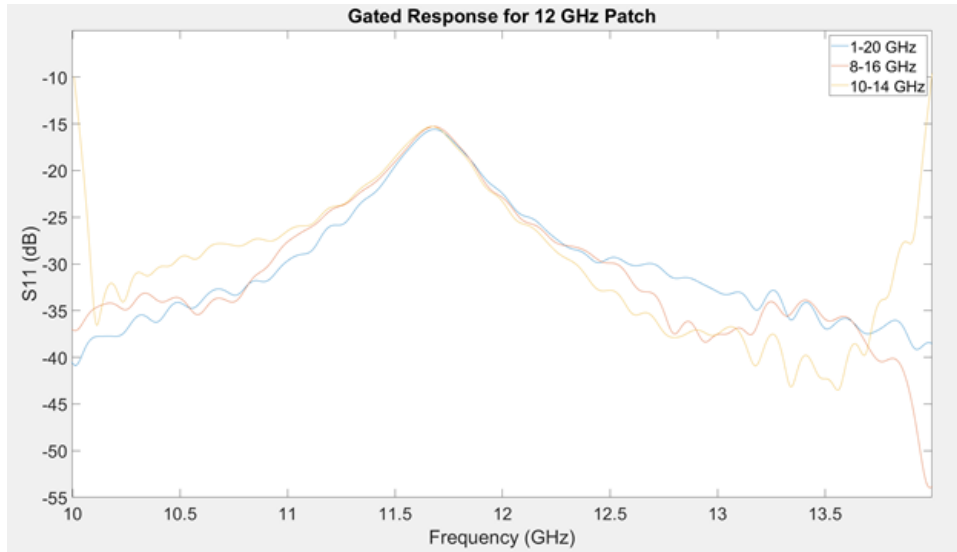
Figure 2.2: Plot showing the different frequency span calibrations on the resonance of the same patch

2.3 Horn Antenna

Using the 10GHz resonator as the test sample, the measurements are performed using three different horn antennas. A 10dB gain X-band horn antenna (7-14 GHz operating frequency), a 15dB gain horn antenna (7-14 GHz operating frequency), and a double-ridge wideband horn antenna (2-18 GHz operating frequency). Fig. 2.3 shows pictures of each antenna tested.

The results are shown in Fig. 2.4, the 10dB gain horn antenna was the best performing for the sensing environment and the size of patch being used, assuming the resonator has resonance between 7

Figure 2.3: (a) 10 dB gain x-band horn antenna. (b) 15 dB gain x-band horn antenna (c) double-ridge wideband horn antenna

and 14 GHz. For this reason, the sensors used for long distance/high temperature were all designed to have a resonance in this range.
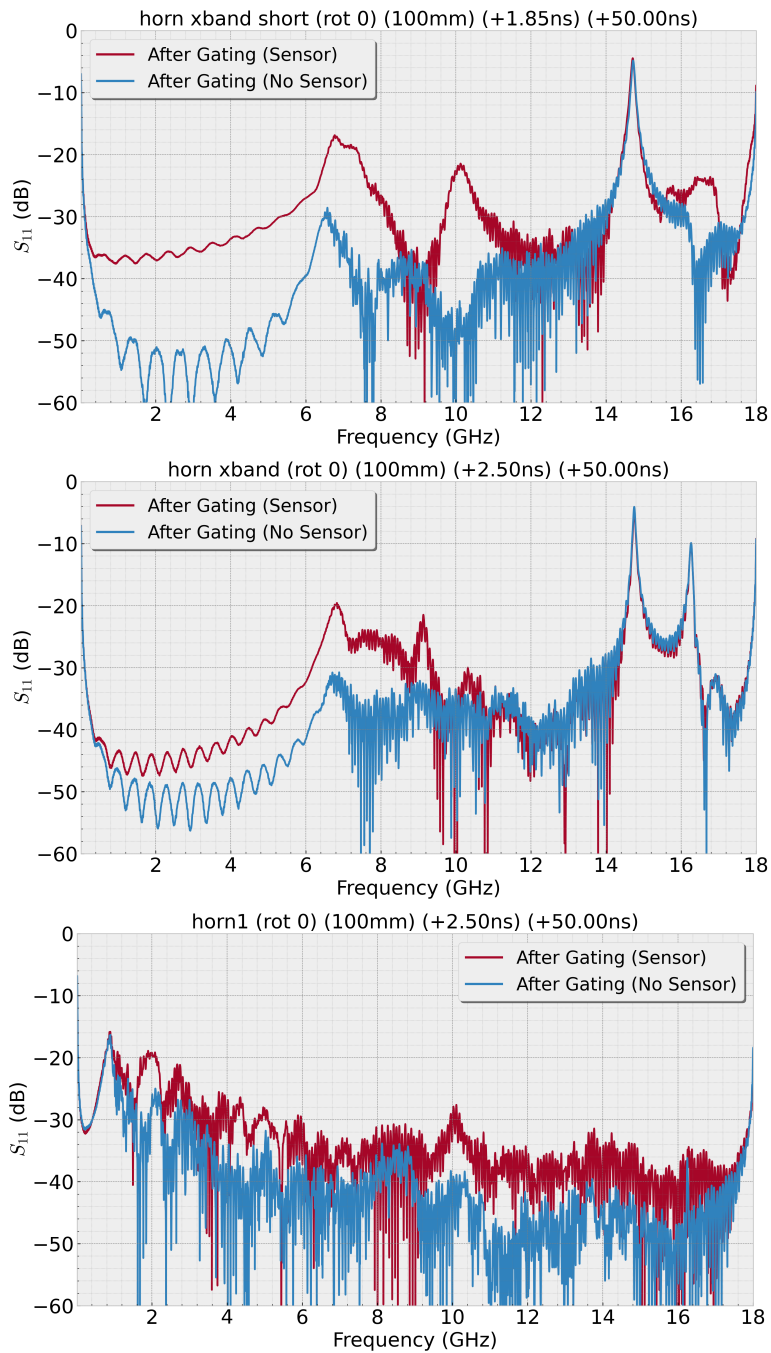
Figure 2.4: (a) 10 GHz resonator response interrogated by 10 dB gain x-band horn antenna. (b) 10 GHz resonator response interrogated by 15 dB gain x-band horn antenna (c) 10 GHz resonator response interrogated by double-ridge wideband horn antenna

CHAPTER 3: REFLECTIVE PATCH SENSORS AT ROOM TEMPERATURE

In [2] the idea of reflective patch temperature sensors using alumina as the dielectric substrate is explored, with platinum as the patch metal and ground plane metal. The findings showed that these alumina sensors could be fabricated and tested up to 1000°C. This design is replicated in simulation first using a silver reflective patch, alumina dielectric, and aluminum ground plane to establish a baseline for future sensor designs based on different dielectrics and conductive ground planes. The idea of a YSZ dielectric sensor is explored as it is a material that is readily available due to being used as a thermal barrier coating for the combustion turbines. The dielectric constant of this material can vary widely, as in [6]. To find the dielectric constant, the resonance is measured and then a sweep of dielectric constants are simulated to match which one corresponds to the measured resonance. Nickel-Chromium-Aluminum Yttrium (NiCrAlY) is a bond coat that is used to improve the adhesion of the dielectric to the conductor below, especially at higher temperatures. Due to this material being in direct contact with the dielectric it can become the ground plane and the effects of this design on the performance of the sensors is also investigated.

3.1 Alumina Sensors

Now that the design from [2] has been replicated and the design considerations identified, the first alumina sample is chosen. A0-4 was chosen with a substrate thickness $h = 0.3$mm. The reason this sample was chosen is because it is roughly half the thickness of the previously simulated design. To maintain the same aspect ratio, the patch resonant length L is halved, and a patch of $L = 4.5$mm is chosen. This design is simulated again and interrogated by a parallel plate ideal waveguide. A sweep is performed on the width, and from the results, a patch width of 4 was chosen. The

Figure 3.1: (a) the metallization process. (b) the finished A0-4 reflective patch sensor.

silver paint was deposited on the substrate by first creating a mask with clear tape over the sample, measuring and cutting the shape of the patch out, and depositing the paint onto the exposed space, and allowing it to cure for 30 minutes at room temperature. The photo of this process and the finished A0-4 sample is presented in Fig. 3.1a and 3.1b respectively.

The simulation is then refined to include the waveguide probing measurement at a distance of 7mm, the same distance used in the physical waveguide measurement. Fig. 3.2 shows that the expected resonance is just above 12 GHz for a dielectric constant of $\epsilon_r = 9$.

With the information from this plot, the measurement results can be used to find the true dielectric constant of the alumina samples used. The measurement is carried out using a vector network analyzer and a KU-band waveguide of operating frequencies between 9.5 GHz and 19GHz. Fig. 3.3 after performing the time domain gating the resonance is found to be about 12 GHz. For a resonance just below 12GHz, this would be consistent with a dielectric constant for alumina of about 9. This is an important step in the measurement process as it will be the method used to confirm the dielectric constant of the YSZ substrate.

Now that the reflective patch sensor is found to be working, the next step in experimentation is to
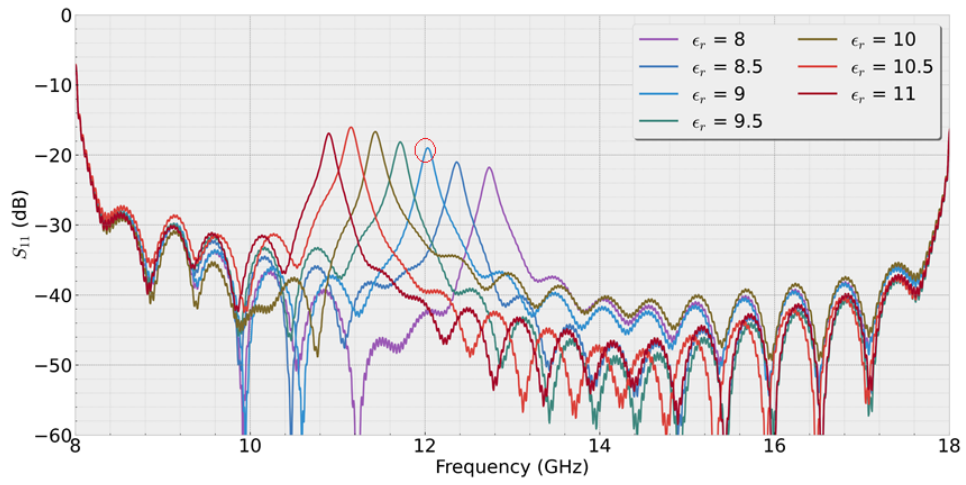
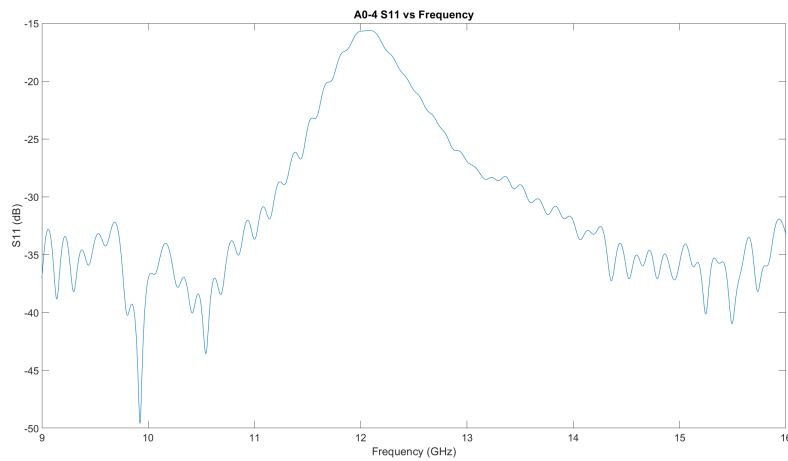Figure 3.2: Simulated sensor responses for multiple ϵ_r values

Figure 3.3: Plot showing S_{11} response for A0-4 sensor after gating.

perform the same test on an alumina sensor using NiCrAlY bond coat.

3.2 Sensors Using Nickel-Chromium Aluminum Yttrium Bond Coat

The NiCrAlY bond coat is used to improve the adhesion of the dielectric substrate to the conductive substrate underneath it, it is especially used for high temperature adhesion. Due to the physics of the reflective patch resonator, assuming the bond coat is not an insulator, the bond coat now becomes the ground plane and due to the difference in conductivity, or potentially the bond coat being a very poor conductor compared to aluminum, the effects of it must be studied. Using HFSS, the effects of different conductivity values for the ground plane on the resonant frequency are studied. In Fig. 3.4 the simulation shows that in order to see a significant change in the resonant frequency, and in the S_{11} of the reflective patch the conductivity must be at least two orders of magnitude lower. From these simulation results, another reflective patch sensor was fabricated
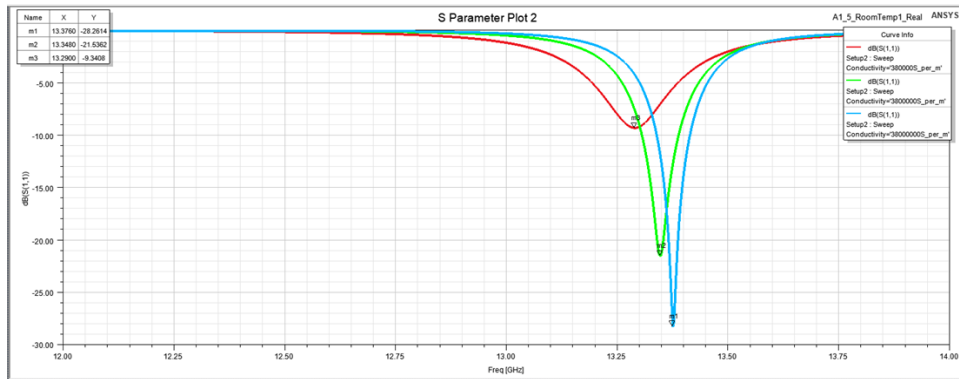
Figure 3.4: Plot showing different conductivities and the effect on the S_{11} response.

using a similar sample, A1-5. Fig. 3.5 shows the metallized A1-5 sample. This sample had very close to the same thickness as A0-4, with a patch designed of the same size. If the bond coat has little to no effect on the measurement, then the bond coat is a decent conductor which is favorable for the operation of the sensor.

After performing the time domain gating, the response shown in Fig. 3.6 there is a very small
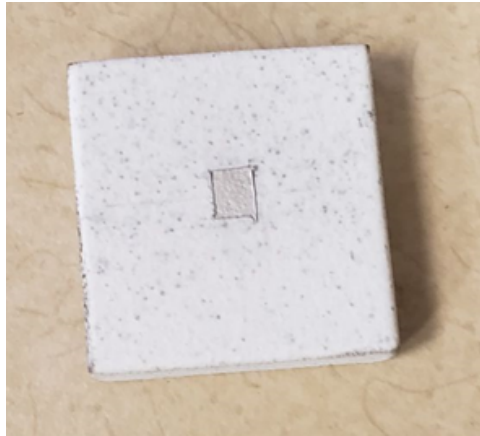
Figure 3.5: Image of the A1-5 sample after metallization.

difference in the resonant frequency, the Q_T of A0-4 is calculated to be about 20. The Q_T of A1-5 is calculated to be about 55. The A0-4 sensor patch was much more roughly fabricated and the patch edges were not very sharp. This contributed to a lowered Q value. However, it is very encouraging to find that the NiCrAlY bond coat is in the same order of magnitude, and also higher performing, in terms of quality factor to the sample that is adhered straight onto the aluminum block underneath. Referring back to Fig. 3.4, these results from the A1-5 sample show the NiCrAlY is at the very least within 1 order of magnitude of the conductivity of aluminum. The performance of the NiCrAlY bond coat at different temperatures with A1-5 is studied in Section 4.1, but first the next step in sensor design is to create a similar design using YSZ as the dielectric constant, as well as perform material characterization to find the dielectric constant of the YSZ being used.
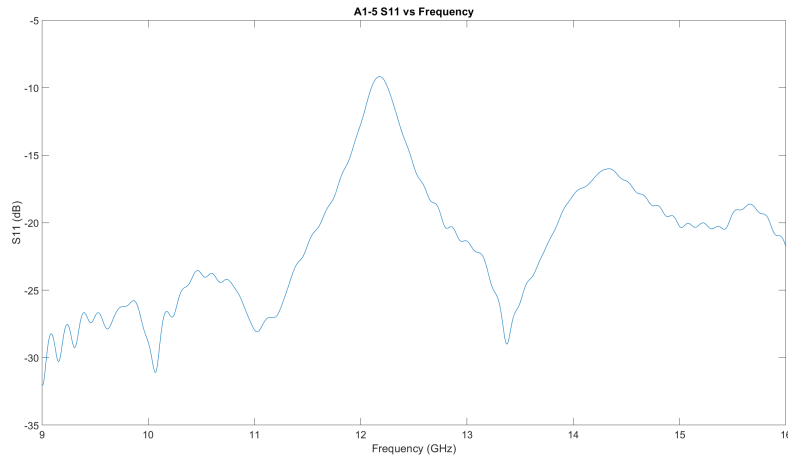
Figure 3.6: Plot showing the S11 response of the A1-5 sample with NiCrAlY bond coat

3.3 Yttrium-Stabilized Zirconia Sensors
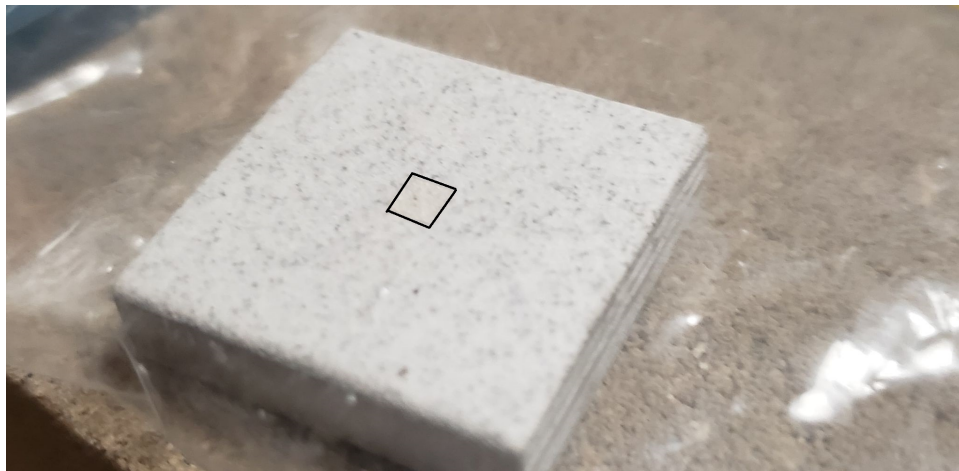
Figure 3.7: Picture of the Y1-1 sensor with silver reflective patch.

YSZ is a ceramic material used as a thermal barrier coating inside of combustion turbines. This material is readily available and if it would serve as a good performing dielectric for the wireless temperature sensor it would offer an effective, practically no cost design to be used in combustion

turbines. Since the NiCrAlY bond coat has proven to perform well as a ground plane, the YSZ sensor is fabricated with the bond coat. Before this material can be used in a final design its dielectric properties must be characterized. According to [6] the dielectric constant of YSZ can vary between 4 and 120.
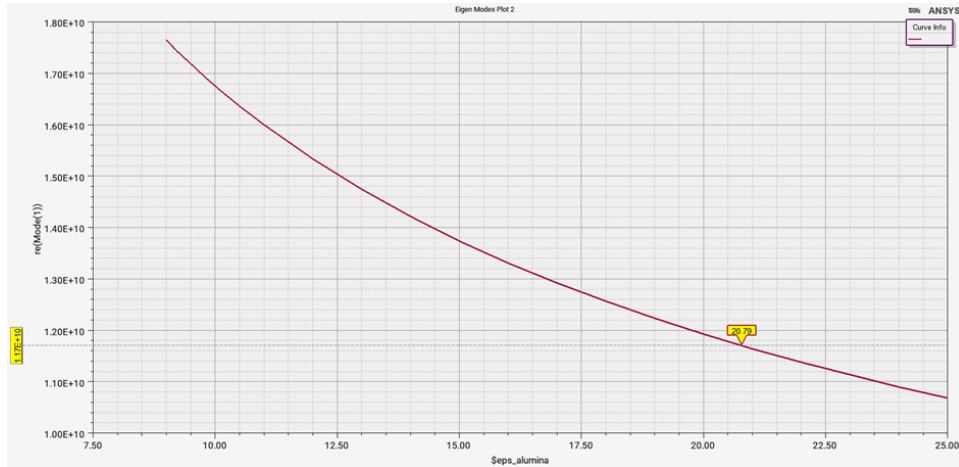
Figure 3.8: Dielectric constant vs frequency plot showing the dielectric constant corresponding with the Y1-1 response from Fig. 3.10

A sample is fabricated using the Y1-1 sample with h = 0.162 mm and a patch made of silver paint (L = 3.5mm) as an initial test of the performance of YSZ sensors in detecting temperature differences. This sample is pictured in Fig. 3.7. The resonant frequency is measured at room temperature and the hot plate measurement is used to confirm the resonant peak moves with the changing temperature. The resonant frequency vs dielectric constant in Fig. 3.8 shows that the dielectric constant of YSZ is estimated to be 21. This experiment is set up by placing the sensor on a hot plate as shown in Fig. 3.9 and setting the hot plate to a temperature of 500°C. A k-type thermocouple is placed in contact with the dielectric of the sensor. Due to the inability to control the temperature of the environment the sensor itself is not actually at the same temperature as the hot plate, but this experimental setup is used only to determine if the YSZ reflective patch

sensor can actually function as a temperature sensor. The resulting measurements from the VNA in Fig. 3.10 show that as temperature increases f_r decreases. This relationship is further explored in Section 4.2.

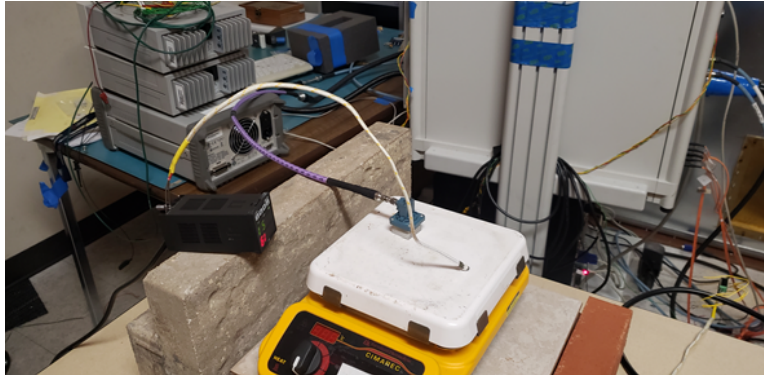Figure 3.9: Hot plate measurement setup. The waveguide is held above the sensor. In the image, the thermocouple is not shown in contact with the sensor, but in practice the thermocouple is placed in contact.
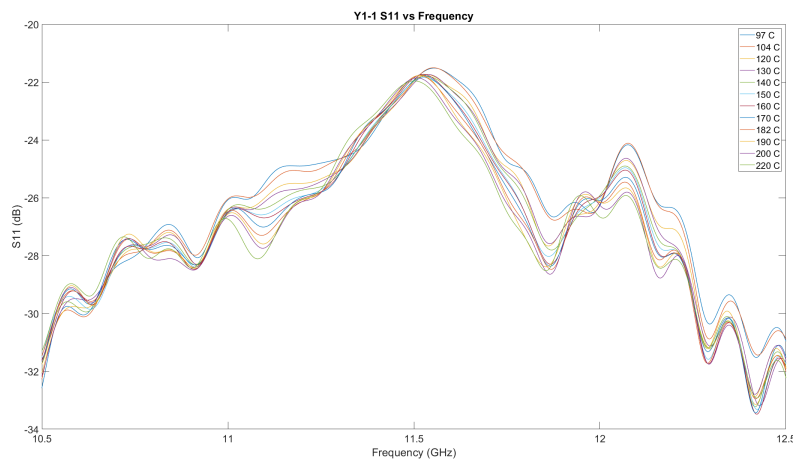
Figure 3.10: Plot showing Y1-1 sensor responses at different temperatures.
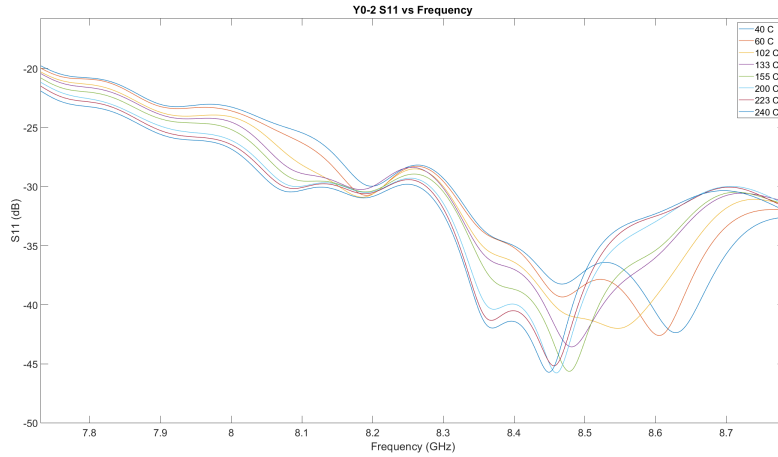
Figure 3.11: Plot showing Y0-2 sensor responses at different temperatures.

To ensure accurate characterization of the YSZ material itself, and attempting to account for any effects the NiCrAlY bond coat may have on the material, a Y0 sample is also fabricated with patch dimensions of 4 mm x 3.1 mm. The same hot plate measurements are performed on the Y0 sensor to characterize its resonance. Fig. 3.11 shows the sensor's response at different temperatures up to 240°C. From simulations in HFSS, the dielectric constant required for a patch to resonate at 8.3 GHz with these dimensions is around 21. Fig. 3.12 shows the results of a sweep of the dielectric constant for the Y0 sensor. If the sensor's dielectric constant were slightly higher, it could be exciting another mode in the patch. This patch size on this material is unideal for operation as a temperature sensor, but for the purposes of material characterization it is acceptable. With the dielectric constant of YSZ characterized, the sensors fabricated for higher temperatures are ready to be metallized.

22

Figure 3.12: Simulation results for a sweep showing the dielectric constant for the Y0 sample.

CHAPTER 4: REFLECTIVE PATCH SENSORS AT HIGH TEMPERATURES

The next step in the design process is to test the sensors at high temperatures close to/above 1000°C. The melting point of alumina is 2072°C, for YSZ the melting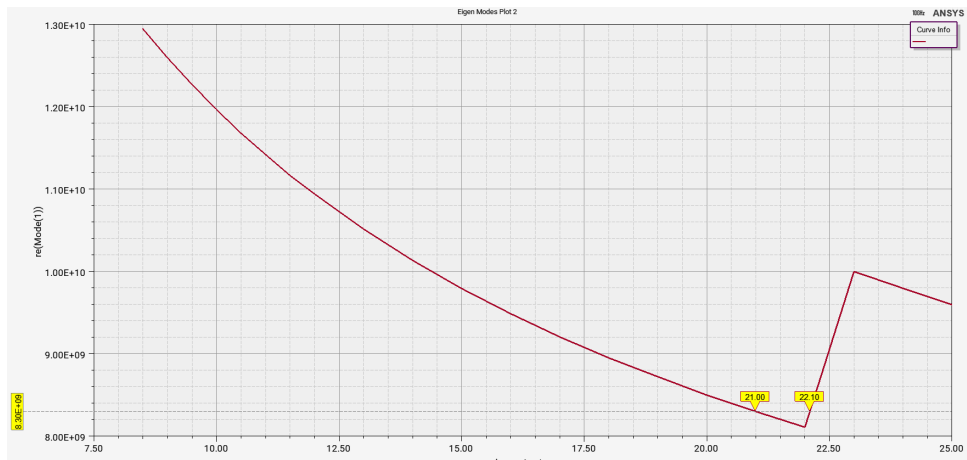 point is around 2700°C. The two types of conductor substrates on the bottoms of these samples are made of HastelloyX (HX), a metal alloy which has a melting point of about 1360°C, and platinum, which has a melting point of 1700°C. The NiCrAlY bond coat has a melting point of 1400°C [7]. These materials are perfect for use at the target temperatures of 1000°C to 1300°C. The bond coat and YSZ have also both proven to perform well as materials the sensor can be composed of. Multiple sensors are tested for high temperature function once again with alumina and YSZ as the dielectric materials used. The sensors are tested at high temperatures and long distances to understand how much flexibility there is with interrogation of the reflective patch sensor. Two types of tests are performed. One is on the A1 and Y1/Y0 samples with a hot plate. Due to the relatively low melting point of the aluminum substrate the sensors are fabricated on, these sensors are heated to much lower temperatures on a hot plate. This is primarily done to test if the YSZ/YSZ+NiCrAlY and alumina+NiCrAlY sensors will work at higher temperatures. The second test is performed using a MHI 2" HeatPad to heat the PA, PY, and A3 sensors to temperatures close to 1000°C.

4.1 Alumina Sensors

The first temperature test performed is on the A1-5 sample using the hot plate configuration from Fig. 3.9. The sample is heated to a temperature of around 240°C on the hot plate. This ensures enough temperature variation to observe the relationship between f_r and temperature, as well as the performance of NiCrAlY as a ground plane conductor. Fig. 4.1 shows the response for the

24
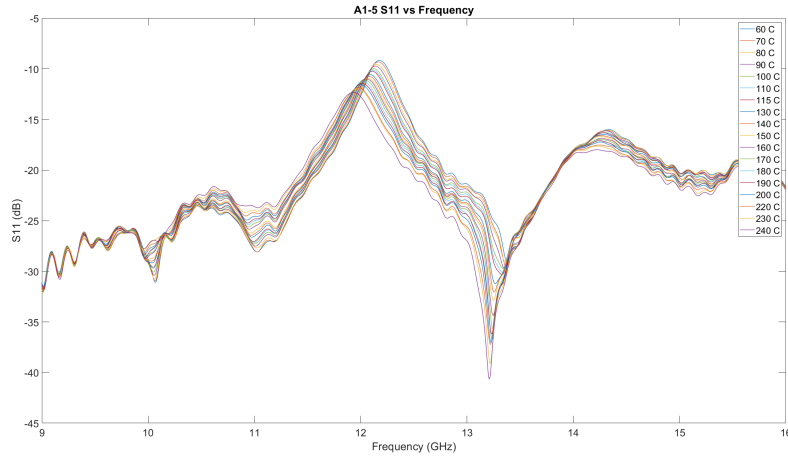
Figure 4.1: Plot of S_{11} response vs Frequency for A1-5 at different temperatures.

sensor at different temperatures.

The relationship between f_r and temperature is plotted in Fig. 4.2 showing a monotonic, almost linear decrease in f_r with an increase in temperature. This is in line with previous research done in [2] and [3]. From the slope of this line, the sensitivity of this sensor, or the sensitivity of the equipment used to measure its response, can be approximated to be 0.0014 GHz/°C, or 1.4MHz/°C.

Figure 4.2: Plot showing the relationship between f_r and temperature.

There are two types of alumina sensors fabricated with a metal substrate intended for very high temperature measurements. One type, PA, is fabricated using HX as the base substrate. This nickel based metal alloy is capable of withstanding temperatures of close to 1300°C without melting. The patch is formed using platinum paste that is sintered at 1000°C in a box 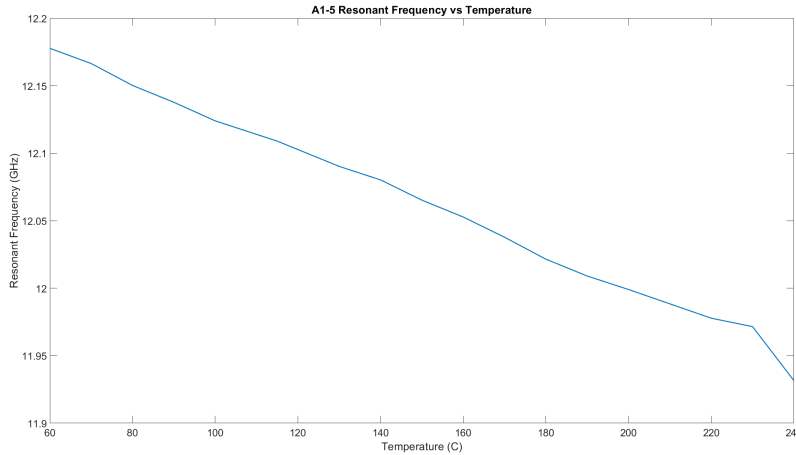oven. The second type, A3, uses platinum as both the patch metal and ground plane. NiCrAlY bond coat is used to adhere the HX to the alumina substrate. Since the bond coat has shown to not significantly affect the performance of the room temperature sensors, it is now tested as a reflective patch material. If it still performs well as a reflective patch material, then that means the material is confirmed to be conductive. Fig. 4.3 shows an image of the PA sensor, and Fig. 4.4 shows an image of the A3 sensor.

Due to the surface area of the PA sensor, and the size of the heating aperture, the PA sample had to be cut to a size that would fit within the 2" diameter heating pad. The PA sensor is placed in the heating pad, where the temperature would be slowly increased to a temperature of 1000°C. The PA sensor's response did not show any resonance. Multiple attempts were made to obtain resonance

26

Figure 4.3: Image of PA sample with sintered platinum paste patch before being cut to fit inside the heating pad.

Figure 4.4: Image of the A3 sample with diffusion bonded platinum patch
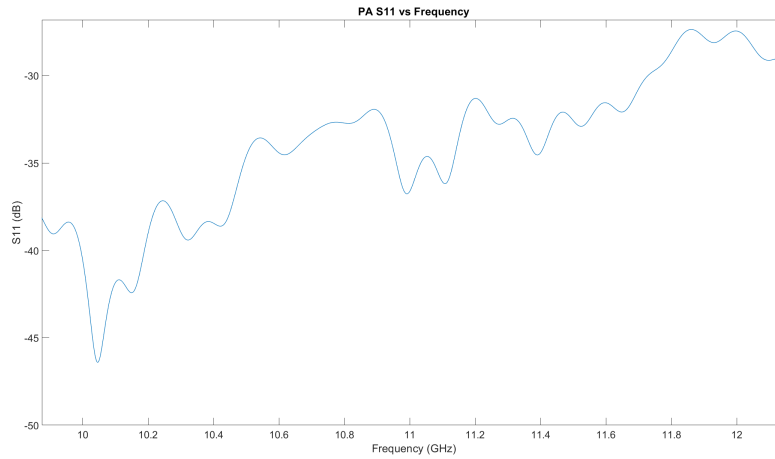
Figure 4.5: Plot showing the response from interrogating the PA sensor. Although there appears to be some kind of peak near 11GHz, this peak is present when rotating the sensor to excite the other mode.

from the PA sample, but regardless of changing patch dimensions or distance to the interrogating waveguide it never showed any resonance. Fig. 4.5 shows the response from interrogating the PA sensor with a 5.1mm x 4.3mm patch. For the TM_{010} mode the resonant frequency should be around 11 GHz, but it was not present.

The heating pad testing is performed on the A3 sample. Its response vs frequency is shown in Fig. 4.6 and from its frequency vs temperature performance in Fig. 4.7 the sensitivity is determined to be 1.2 MHz/°C. This is consistent with the sensitivity observed from the A1-5 sensor, showing promising agreement between sensors fabricated with and without the NiCrAlY bond coat.
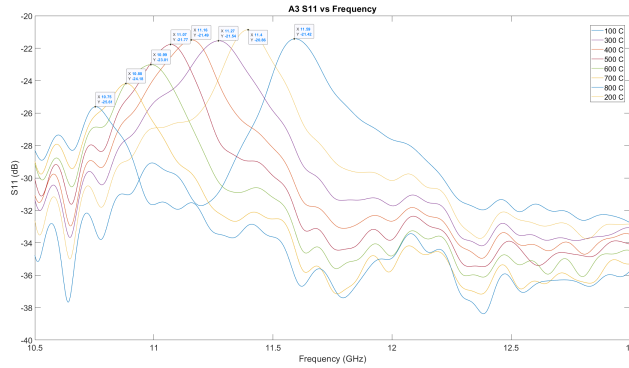

Figure 4.6: Plot of S_{11} vs frequency for the A3 sensor at different temperatures.
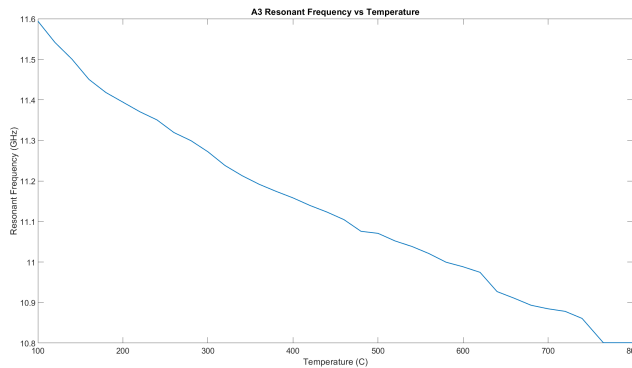

Figure 4.7: Plot of the relationship between f_r and temperature for the A3 sensor.

29

4.2 Yttria-Stabilized Zirconia Sensors

The Y1-1 and Y0-2 sensors previously studied in Section 3.2 were tested in the same hot plate measurement setup used for the A1-5 sample up to the same temperature. The only difference between these two experiments are the sensors used. The response for Y1-1 is shown in Fig. 3.10. The f_r vs temperature plot is shown in Fig. 4.8. From this relationship, the sensitivity of the YSZ sensor is calculated to be 0.4 MHz/°C. The YSZ material is not as sensitive to temperature change as the alumina.
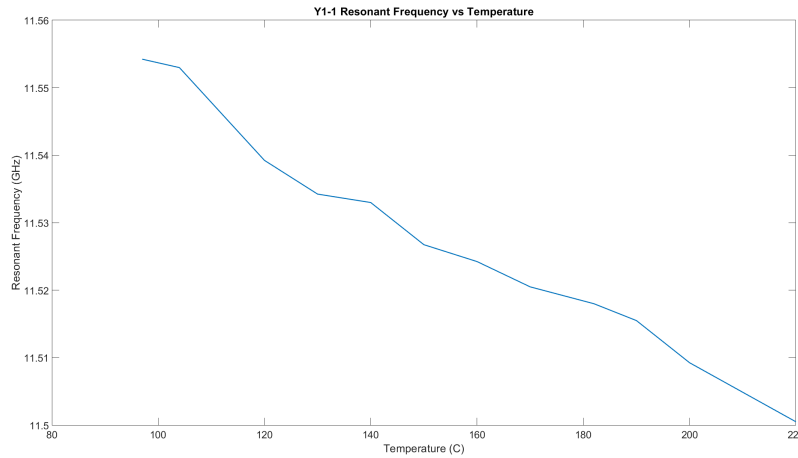
Figure 4.8: Plot showing the relationship between f_r and temperature for the YSZ sensor Y1-1.

To isolate any effects on the sensor from the NiCrAlY bond coat, the Y0 sensor was also tested. This sensor's response was shown in Fig. 3.11, and its f_r vs temperature relationship is shown in Fig. 4.9. The sensitivity of this sensor is calculated to be about 0.07 MHz/°C, which is roughly 20% of the sensitivity of the Y1-1 sample, which suggests the bond coat is interacting with the material in some way and affecting its electrical properties.

To ensure that these results were not caused by any differences in the patch conductor (copper tape
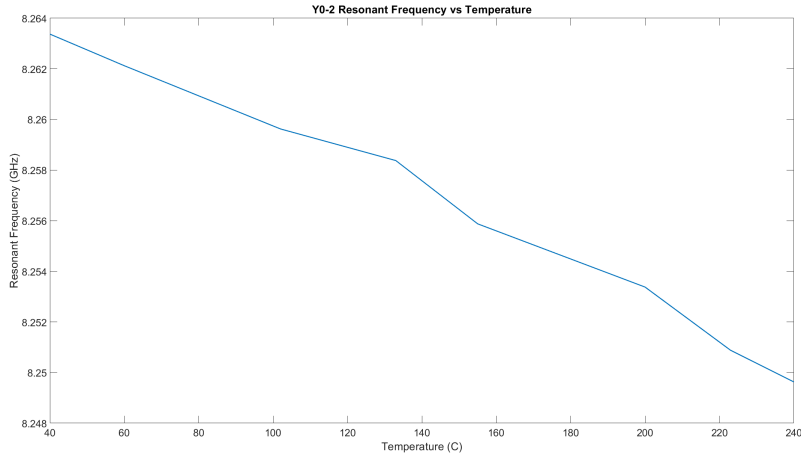
Figure 4.9: Plot showing the relationship between f_r and temperature for the YSZ sensor Y1-1.

vs conductive silver paint) another patch was fabricated on another Y0 sample (Y0-4) to check against the copper tape. The resulting patch was slightly larger and to ensure the resonance could be measured, it was measured with an OEWG with an operating frequency of 5GHz - 10 GHz. This patch was measured to have a resonant frequency of about 7.55 GHz, although the peak is not very sharp or well-defined. The same hot plate measurement was performed and the results are shown in Fig. 4.10 and Fig. 4.11.

Figure 4.10: Plot showing the response of the Y0-4 sensor
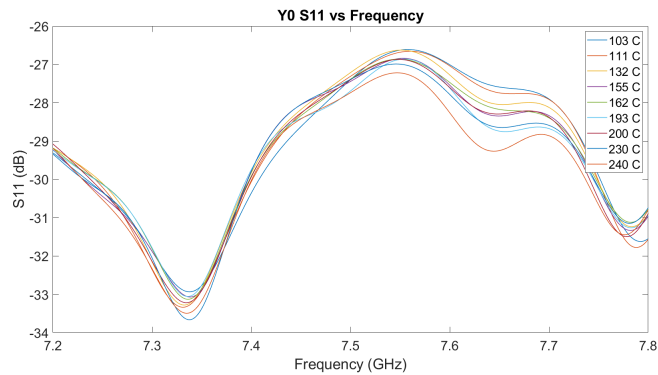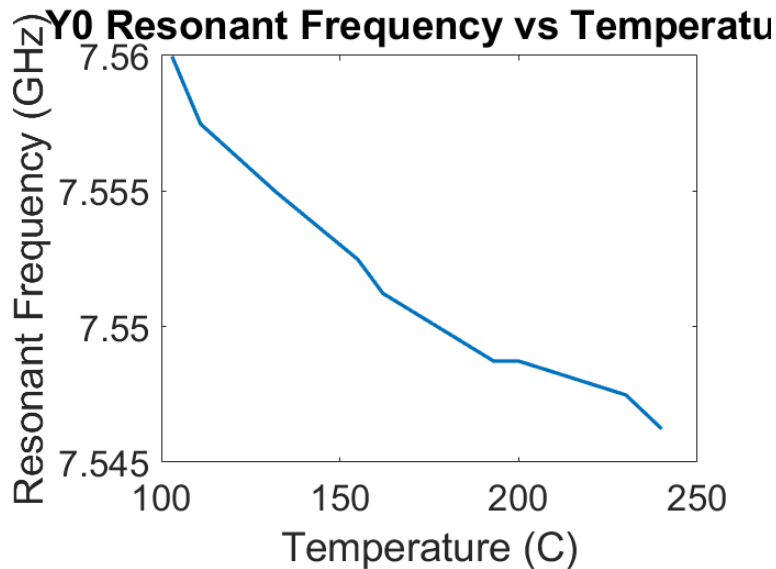
Figure 4.11: Plot showing the relationship between f_r and temperature for the Y0-4 sensor.

The sensitivity was calculated to be 0.1 MHz/°C, which is close to the sensitivity of the other Y0 sample, but still only 25% of the sensitivity of the Y1 sample. Both suggest that sensors with only YSZ as the dielectric substrate do not operate very well, and even when the Y1 is compared to alumina it still suggests better performance from the alumina. The PY sensor was fabricated with a platinum paste patch in the same way as the PA sensor. Fig. 4.12 shows an image of the PY sensor after being cut to fit in the heating pad. Much like the PA sensor, the PY sensor would not show a resonant frequency regardless of patch dimensions, waveguides used, or network analyzer used. As shown in Fig. 4.13 for a dielectric constant of around 20, the expected resonant frequency for this patch should have been around 6GHz. Although there does appear to be some sort of peak close to 6GHz, this peak is present when the sensor is removed, and also when the sensor is rotated. This suggests some interaction/reaction with the NiCrAlY bond coat and HX material may be causing these materials to not function as proper ground plane conductors. Although the PY sensor could not be measured, the Y1 and Y0 samples still provide meaningful results for the possibilities of using YSZ as a dielectric for a wireless temperature sensor.

32
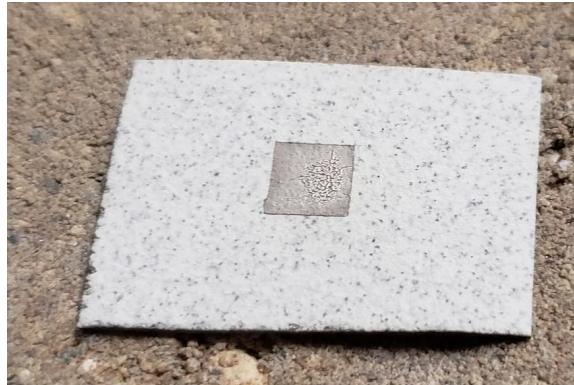
Figure 4.12: Image of the PY sensor with platinum sintered patch.
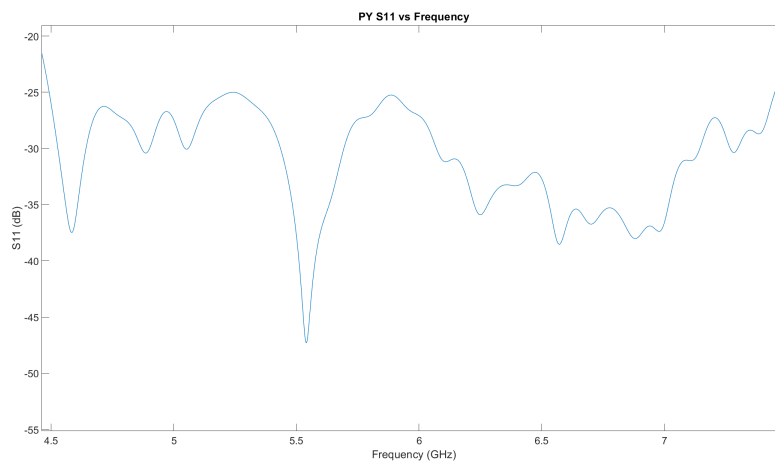
Figure 4.13: Response shown on the PNA while interrogating PY sample.

4.3 Long Distance Measurements

For operation inside a harsh environment it is important to be able to interrogate and measure the response from the sensor from a safe distance for the interrogating antenna. To measure sensing distance three types of reflective patch resonators are tested by using a 10dB gain x-band horn antenna to interrogate them. The first type of resonators are copper patches on Rogers 4003 substrate.

Figure 4.14: Measurement setup using 10dB gain x-band horn antenna to interrogate sensors inside antenna chamber.

These resonators have a high Q and each one is designed to resonate at different frequencies, 10 GHz, 12GHz, and 14 GHz. The 10GHz resonator was measured inside an antenna chamber at various distances. The measurement setup shown in Fig. 4.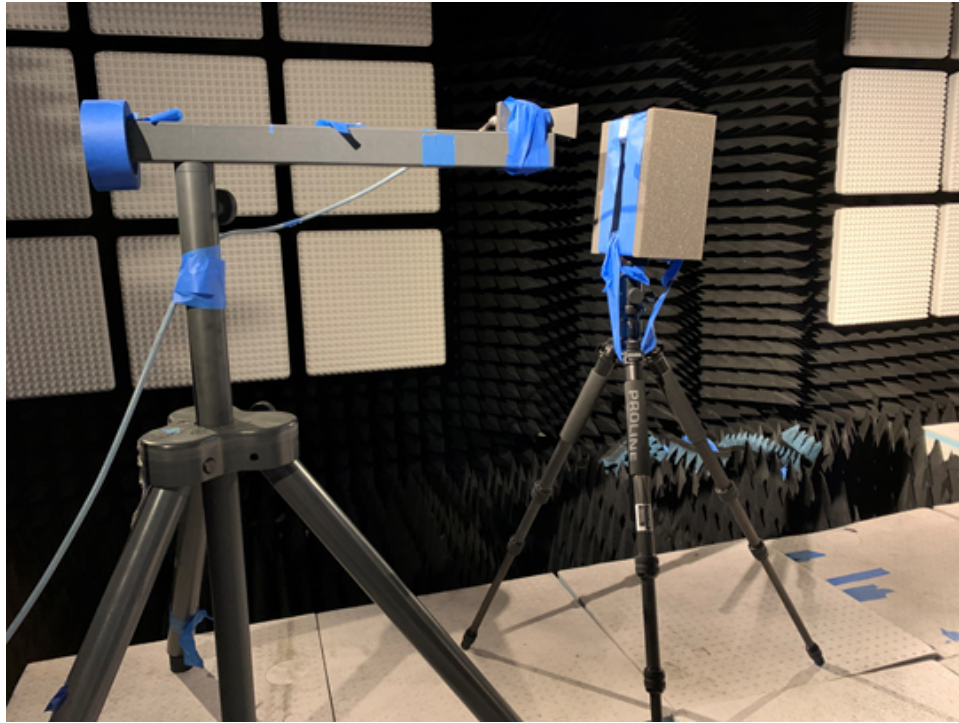14 was used to test the performances of the resonators and sensors at long distances up to 30 cm. The effects of significantly long distance measurements on the response of the resonator are shown in Fig. 4.15. The resonant frequency f_r does not change with sensing distance, but the S_{11} level goes down the further the sensor is from the interrogating antenna. The second resonator under test is the alumina sample A3 used in high temperature measurements. This sensor's response is measured at a few distances Fig. 4.16, the maximum distance where the resonance can still be measured by the 10dB gain horn antenna is between 6 and 9 cm, showing promising results for possible uses within a combustion turbine engine.
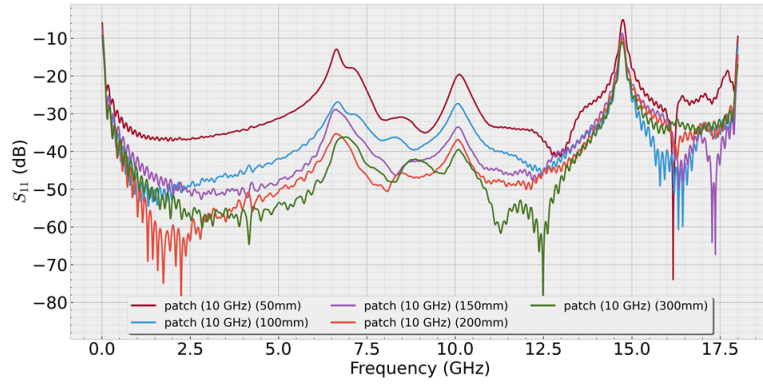
Figure 4.15: Plot showing the 10 GHz resonator response at long distances.
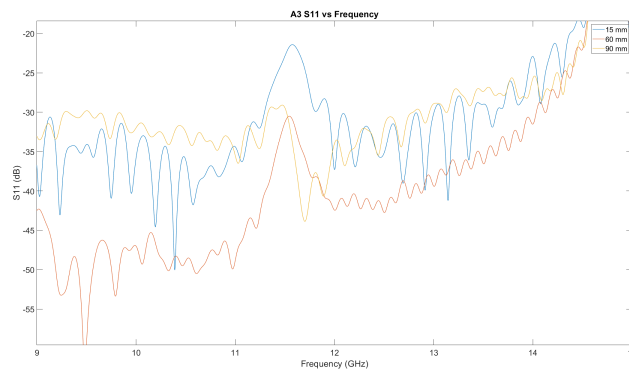

Figure 4.16: Plot showing S_{11} response for A3 sensor at various distances. The peak is no longer visible at 9cm.

CHAPTER 5: CONCLUSION

Several wireless temperature sensors based on a reflective patch have been demonstrated for high temperature environments. By introducing YSZ as a dielectric material it offers an alternative dielectric that is already in use as a thermal barrier coating for combustion turbines, reducing the costs of fabrication. Introducing NiCrAlY bond coat as a ground plane conductor presents a design that is more robust for high temperature environments, ensuring that the adhesions will remain intact. These temperature sensor designs build upon the previous simple design, and continues to be a low-profile, easy to fabricate temperature sensor suitable for a vast amount of applications including within combustion turbines. Through the results from the PA and PY sensors, it was found that the bond coat and HX do not work well together when used as the ground planes for the sensors. As a summary of the findings of the various sensors, Table 5.1 shows the sensors, the materials they are composed of, and their temperature sensitivities. Sensors that did not work or were not tested at higher temperatures are labeled "N/A."

Table 5.1: Sample names, their composition, and their sensitivity.

Sample	Composition	Sensitivity
A0-4	Silver Patch, Alumina, Aluminum	N/A
A1-5	Silver Patch, Alumina, NiCrAlY, Aluminum	1.4 MHz/°C
Y0-2	Copper Patch, YSZ, Aluminum	0.07MHz/°C
Y0-4	Silver Patch, YSZ, Aluminum	0.1 MHz/°C
Y1-1	Silver Patch, YSZ, NiCrAlY, Aluminum	0.4MHz/°C
PA	Platinum Patch, Alumina, NiCrAlY, HX	N/A
PY	Platinum Patch, YSZ, NiCrAlY, HX	N/A
A3	Platinum Patch, Alumina, Platinum Ground	1.2MHz/°C

5.1 Future Work

Future research will include effects of turbine movement, such as metallic obstacles and change in incident angle of the interrogating signal, on the performance of the sensor. The possibilities of using a circular reflective patch and study the effects of using circular, rather than linear, polarization on the effects of the sensor's performance. This is especially interesting considering the turbine movement. Future research should also adapt more sophisticated detection techniques to significantly improve the signal-to-noise ratio of the signal coming from the sensor, which will result in higher rates of detection and better performance. Future research would also go into a deeper characterization of the electrical properties of the NiCrAlY bond coat and a closer look into the effects it has on sensor performance.

LIST OF REFERENCES

[1] U.S. Dept. of Energy, Office of Fossil Energy, *How Gas Turbine Power Plants Work* Energy.gov. [Online]. Available: https://www.energy.gov/fe/how-gas-turbine-power-plants-work. [Accessed: 07-Apr-2021].

[2] H. Cheng, *Integrated Microwave Resonator/antenna Structures for Sensor and Filter Applications*,(2014). Electronic Theses and Dissertations, 2004-2019. 6675. https://stars.library.ucf.edu/etd/6675

[3] S. Fargeot, D. Guihard, and P. Lahitte, *Dielectric characterization at high temperature (1600° C) for space applications*,in Proc. IEEE Int. Conf. Microw. Technol. Comput. Electromagn., Beijing, China, May 22-25, 2011 pp. 48-50.

[4] K. K. Karnati, Y. Yusuf, S. Ebadi and X. Gong, *Theoretical Analysis on Reflection Properties of Reflectarray Unit Cells Using Quality Factors*, in IEEE Transactions on Antennas and Propagation, vol. 61, no. 1, pp. 201-210, Jan. 2013, doi: 10.1109/TAP.2012.2214753.

[5] Fouliard, Quentin, *Characterization of Rare-earth Doped Thermal Barrier Coatings for Phosphor Thermometry* (2019). Electronic Theses and Dissertations, 2004-2019. 6869. https://stars.library.ucf.edu/etd/6869

[6] Lim, Geunsik, and Aravinda Kar. *Radiative properties of thermal barrier coatings at high temperatures.* Journal of Physics D: Applied Physics 42.15 (2009): 155412.

[7] American Elements, "Nickel Chromium Aluminum Yttrium Alloy", NICR-ALY-01 datasheet, May 2015.